Variability in growth and tissue composition (CNP, natural isotopes) of the three morphotypes of holopelagic Sargassum

T. Changeux, L Berline, W Podlejski, T Guillot, Valérie Stiger-Pouvreau, S Connan, T Thibaut

Title.

Distinct growth and tissue composition (CNP, natural isotopes) of the three morphotypes of holopelagic *Sargassum*

Authors names and affiliations.

Changeux T. (ORCID 0000-0002-0418-3321); e-mail : thomas.changeux@ird.fr; Affiliation: Mediterranean institute of oceanography (MIO); Postal address: Institut Méditerranéen d'Océanologie (MIO) - Equipe 5 EMBIO, Campus de Luminy, Case 901, Océanomed, Bât. Méditerranée 26M/102, 13288 Marseille Cédex 9

Berline L. (ORCID 0000-0002-5831-7399); e-mail: leo.berline@mio.osupytheas.fr; Affiliation: MIO

Podlejski W. (ORCID 0000-0002-3286-4984), e-mail: witold.podlejski@mio.osupytheas.fr; Affiliation: MIO

Guillot T., e-mail: tymguillot@gmail.com; Affiliation: Ifremer Martinique, 79 route de Pointe Fort 97231 Le Robert

Stiger-Pouvreau V. (ORCID 0000-0003-3041-0468), e-mail: valerie.stiger@univ-brest.fr; Affiliation: LEMAR Technopôle Brest-Iroise, rue Dumont d'Urville, 29280 Plouzané.

Connan S. (ORCID 0000-0002-8280-1041), e-mail: solene.connan@univ-brest.fr; Affiliation: LEMAR

Thibaut T. (ORCID 0000-0001-8530-9266); e-mail: thierry.thibaut@univ-amu.fr; Affiliation: MIO

Corresponding author

Changeux T. e-mail : thomas.changeux@ird.fr; Affiliation: MIO

Highlights

- *Sargassum fluitans* III growth rate is the highest.
- *Sargassum natans* I growth rate is the lowest.
- Tissue composition differs between morphotypes.

Abstract

Holopelagic *Sargassum* blooms in the tropical North Atlantic since 2011 are composed of two species, *Sargassum natans* and *S. fluitans*, and three morphotypes: *S. natans* VIII, *S. natans* I and *S. fluitans* III. The distinct morphology and the variations in space and time of the proportion of these three morphotypes suggest that they may have different physiology. For the first time, we have quantified the growth rates of these three morphotypes through *in situ* 9-day experiments on the coast of Martinique Island (French West Indies). Despite the non-optimal conditions for growth for these pelagic species, we have observed that *Sargassum fluitans* III was growing faster (approximately twice as fast) than *S. natans* VIII and *S. natans* I. *S. natans* I exhibited the slowest growth. The differences in tissue composition (CNP and CN natural isotopes) of morphotypes point to a greater benefit for *S. fluitans* III from the coastal localization of our experiment than for the two *S. natans* morphotypes, and suggest that *S. natans* I had achieved its last growth further offshore before our experiment. These contrasting growth performances are consistent with the dominance of *S. fluitans* III in recent observations in the Caribbean. This also makes this last morphotype the best candidate for cultivation. Making the distinction between the growth performances of morphotypes may improve the current predictive models.

Keywords

Holopelagic *Sargassum*, Morphotypes, Sargasso, Growth, Nutrient content, Natural isotopes

1. Introduction

Since 2011, the tropical North Atlantic Ocean has been the site of seasonal blooms of holopelagic *Sargassum*, rooted in the North Equatorial Recirculation Region. Holopelagic *Sargassum* are currently forming the Great Atlantic *Sargassum* Belt that can be observed from space (Wang et al., 2019), and causes strandings westwards, along the whole of the North Atlantic coast of South America and the Caribbean area, including the Gulf of Mexico, and eastwards along the West African coasts (Berline et al., 2020).

These strandings are composed of three distinct morphotypes: *Sargassum natans* VIII Parr, *S. natans* I Parr, and *S. fluitans* III Parr (Schell et al., 2015). Each morphotype shows a distinct morphology especially blade size, number of blades and air bladders (floats) per stem, and presence of thorns on the stem (García-Sánchez et al., 2020; Schell et al., 2015) suggesting that the three morphotypes may have different biological characteristics.

Since the beginning of *Sargassum* blooms in 2011, significant variations of the abundance in morphotype composition have been observed. Initially, S. *natans* VIII was dominant in the south (Antilles Current, Eastern Caribbean and Western Tropical Atlantic) and *S. natans* I in the north (south of the Sargasso Sea) (Schell et al. (2015) November 2014 to May 2015). In 2017, during two open ocean campaigns along a latitudinal gradient from Guyana to the Sargasso Sea (https://doi.org/10.17600/17004300) and following a longitudinal transatlantic route (https://doi.org/10.17600/17016900) from Cabo Verde Island to Guadeloupe, *S. fluitans* III appeared to be dominant north of Guadeloupe for the first cruise and everywhere for the second cruise. More recently, studies have shown a quasi-permanent dominance of *S. fluitans* III in *Sargassum* strandings on Mexican Caribbean shores from 2016 to 2020 (Vázquez-Delfín et al., 2021; García-Sánchez et al., 2020), along the Jamaican coast (Machado et al., 2022), and on the Caribbean, Floridan and Bahaman coasts (Iporac et al., 2022) as well as in the course of a 2022 transatlantic cruise (https://energieaugrandlarg.wixsite.com/website).

Predictive models of *Sargassum* dynamics in the Atlantic (Brooks et al., 2018; Jouanno et al., 2021) use parameters based on physiological studies that do not differentiate between morphotypes (Hanisak and Samuel, 1987; Lapointe, 1995; Lapointe et al., 2014). However in macroalgae, the life traits are often taxon-dependent (Vranken et al., 2022) and therefore could explain the variations in dominance between morphotypes with time and across the North Atlantic. Taking into account differential growth rate may improve the model's simulations.

Differential physiology would also impact tissue composition of *Sargassum* in CNP including C:N, N:P, C:P ratios and $\delta^{13}C$, $\delta^{15}N$ isotopes, as it integrates *Sargassum* environmental history along its drift path (Lapointe et al. 2021, Vázquez-Delfín et al., 2021).

The aim of this work was to quantify the growth rates and tissue CNP composition of the three morphotypes through *in situ* short term experiments in Martinique Island (French West Indies).

1 Materials and methods

1.1 *Location of experimental site and* Sargassum sampling

Experiments were performed on the east coast of Martinique Island, in Baie du Robert, close to the Ifremer marine station, where a meteorological station is located. It took place in May-June 2021, when the Island is frequently supplied with *Sargassum* (Johns et al., 2020). This shallow bay (<30 m depth) faces the Atlantic Ocean and receives *Sargassum* pushed by the northeast trade winds after passing over the continental shelf, which extends for more than 15 km offshore (Fig. S1).

The nutrient concentrations (NO_3^-, NO_2^-, NH_4^+, PO_4^{2-}) of surface seawater in the bay was monitored once every 2 months since 2017 as part of an extension of Ifremer's REPHY network (Belin et al., 2021) to the French overseas territories. The values (mean ± SD) measured at the REPHY station, situated 400 m from our experimental site (S1), were low for a coastal station, especially when considering the different forms of N, NO_3^-+NO_2^- (0.3±0.3 µmole L^{-1}) and NH_4^+ (0.3±0.3 µmole L^{-1}), with

regard to PO_4^{2-} (0.07±0.05 µmole L^{-1}). This absence of pollution is confirmed by a previous detailed study of the bay (De Rock et al., 2019).

1.2 *Growth experiment*

Sargassum individuals were collected off the coast within the bay selecting the young clumps following the criteria of Stoner and Greening (1984) to age the clumps. For each morphotype, we cut fragments of 5 to 20 cm length from the apical part, free from visible epiphytes. To be consistent with field observations, the three morphotypes were grown together. Approximately 20 g of wet weight of each morphotype (5-10 fragments, 60 g in total) hereinafter called a batch, were placed in 5 L transparent plastic bottles, perforated with one hundred holes to allow good water circulation. These bottles were attached to mooring cables at 2 m depth to avoid destruction of the devices by wave effect. Temperature and light inside two of the four bottles was recorded with UA-002-08 (HOBO) data loggers.

The entire experiment lasted 9 days, from May 25th to June 3rd 2021. The wet weight was measured every 3 days. The wet weight of each batch was measured on a BAXTRAN BR balance (0.1 g readability) after dewatering using absorbent paper in a salad spinner. Inside each batch, three individuals per morphotype (n = 36) were identified with colored beads strung on a nylon thread attached to the fragment. The wet weight of each individual (n = 12 per morphotype) was obtained as for the batch but by using a more accurate balance (PRECISA 321LT, 0.1 mg readability). In addition, for each individual the number of floats was counted.

1.3 *Water, tissue, and data analysis*

At the beginning of the experiment, and before each measurement session, we sampled the water in 200 mL plastic bottles to measure nutrient composition. The sample was fixed with 100µL $HgCl_2$ per bottle, and then stored in a cool place protected from light. The analyses were carried out by automated colorimetry for NO_3^-, NO_2^-, NH_4^+, PO_4^{2-} (Aminot and Kérouel, 2007) and for NH_4^+ (Holmes et al., 1999).

At the end of the experiment, eight samples of 5 g wet weight of each morphotype were analyzed for C, N, P, $\delta^{13}C$ and $\delta^{15}N$ tissue composition. These samples were dried in an oven at 60°C during 48 h, reduced into powder, acidified to eliminate mineral sources of carbon, and analyzed by spectrometry following Raimbault et al. (2008).

The growth rate (GR) in weight was calculated in d^{-1} following:

$$GR_d = \frac{1}{d} ln\left(\frac{W_d}{W_0}\right)$$

were d = number of days (d = 9 for the entire experiment) and W_d = wet weight at day d, W_0 = wet weight at day 0.

The floats ratio (FR) was calculated (in %) with reference to the initial number of floats for the entire experiment following:

$$FR = \frac{N_9}{N_0}.100$$

were N_9 = number of floats at day 9 and N_0 = number of floats at day 0.

Non parametric Kruskal-Wallis test (KW test) followed by Dunns post-hoc test were used to test the morphotype effect on *Sargassum* GR, FR and tissue composition with a significance level of 0.05.

2 Results

2.1 *Field conditions*

During the 9 days of the experiment, water temperature inside the bottles varied from 28°C at night to 31°C during the day (06:00-18:00) when light inside the bottle varied from 74 to 740 µmol photons m^{-2} s^{-1} with a mean value of 137 µmol photons m^{-2} s^{-1}. The nutrient concentrations were high and variable compared to REPHY measurements (respectively 1.7 ± 2.0 vs 0.3 ± 0.3 µmole L^{-1} for NO_3^-+NO_2^-, 2.1 ± 1.7 vs 0.3 ± 0.3 µmole L^{-1} for NH_4^+ and 0.3 ± 0.3 vs 0.07 ± 0.05 µmole L^{-1} for PO_4^{2-}).

The daily rainfall, including one day before the start of the experiment, varied from 0 to 10.6 mm, with a mean of 1.52 mm which is below the average of 2.07 mm from May to June 2021 at the station. The wind speed and direction were regular for the season (9.73 $m.s^{-1}$ oriented WNW (67.27°)).

2.2 *Patterns of change in the Sargassum weight and floats ratio*

The increase in *Sargassum* weight in the course of the experiment was clearly visible when considering the batches (Fig. S2). After 9 days, the initial 20 g were exceeded by all morphotypes, reaching about 25 g for *S. natans* VIII and *S. natans* I and approaching 30 g for *S. fluitans* III. After 6 days, the weight increase slowed down for all morphotypes. In contrast, this increase was lower and more variable in the individual measurements (Fig. S2). The floats ratio (FR) after 9 days was overall below 100%, showing a loss of floats for all morphotypes (Fig. S3). This was especially the case for *S. natans* I.

2.3 *Growth rate*

For all morphotypes, the GR over every 3-day period decreased overall over time from the beginning of the experiment (Fig. 1 A). The median value of batch GR varied from 0.063 to 0.022 d^{-1} after 3 days, from 0.044 to 0.018 d^{-1} after 6 days, and from 0.019 to -0.006 d^{-1} after 9 days. *Sargassum fluitans* III had always the highest GR values and *S. natans* I the lowest. *Sargassum natans* VIII GR was intermediate. After 9 days, the individual GR showed a significant variation between morphotypes (KW test χ^2= 16.244, df = 2, p-value = 0.0002969). The Dunns post hoc gives two significant results: *S. fluitans* III vs *S. natans* I (p=0.0000678***) and *S. fluitans* III vs *S. natans* VIII (p=0.0313*). Even if the mean individual GR of *S. natans* I was negative, linked with the first signs of senescence, the mean batch GR of this morphotype was positive (Fig. 1 B).

2.4 *Tissue elemental composition (C, N, P, $\delta^{13}C$, $\delta^{15}N$) of* Sargassum

The effect of morphotype was significant only for %N, $\delta^{15}N$, $\delta^{13}C$ and C:N (Table S1). For other elements, the median values were %C = 23.52%, %P = 0.07%, N:P = 30.33 and C:P = 827.43.

The post hoc Dunn tests (Fig. 2; Table S1) showed that *S. fluitans* III was characterized by a high %N, $\delta^{15}N$ and low C:N and $\delta^{13}C$. In contrast, *S. natans* VIII showed low %N, $\delta^{15}N$ and high C:N and $\delta^{13}C$ and *S. natans* I was essentially characterized by a low $\delta^{15}N$.

3 Discussion

3.1 *Changes in growth performance during the experiment*

For the three morphotypes, GR (0.02-0.04 d^{-1} for batches) were in the low range of literature growth data reported by Brooks et al. (2018), *i.e.* [0.029-0.11] d^{-1} relying on *in situ* (Lapointe 1986, Lapointe et al. 2014) and laboratory experiments (Hanisak and Samuel, 1987). In addition, GR decreased with time for all morphotypes. This does not align with the neritic origin of our samples, generally associated with low nutrient limitation and high GR following Lapointe (1995). These results, for both batches and individuals, indicate that algae were not in optimal growth conditions. This decrease of GR may be due:

- to excessively high seawater temperatures [28-31°C] observed during the experiment, as decrease in growth after 24°C was observed by Hanisak and Samuel (1987) for *S. natans*;
- to light limitation since our mean light measurement of 137 µmol photons m^{-2} s^{-1} in the bottle corresponds to intermediate GR of 0.02 d^{-1} (Hanisak and Samuel, 1987);
- to stress related to the confinement in the bottles despite the numerous holes made in order to renew the water. Pelagic *Sargassum* are known to produce large quantities of dissolved organic carbon (Powers et al., 2019) that promote, together with high nutrient level, bacterial growth (Michotey et al., 2020).

GR did not correspond to maximum growth values, taking into account both the phenomenon of growth and senescence over 9 days. Although culture conditions may be limiting, our results clearly show contrasting performances among morphotypes.

3.2 *Differential growth between the 3 morphotypes and implications*

Sargassum fluitans III was growing faster, approximately twice as fast as *S. natans* VIII and *S. natans* I. This is consistent with lab experiment results of Hanisak and Samuel (1987). Moreover, *S. natans* I exhibited the slowest growth rate. This suggests that morphotypes matter. When exposed to high temperature, high nutrient concentration and a slight light limitation *S. fluitans* III does better than *S. natans* I.

These differences may have implications with regard to the relative abundance of morphotypes observed at sea and in strandings. However GR cannot be simply translated into abundances. The coexistence of the three morphotypes suggests that processes other than growth maintain competitive success of the *S. natans* morphotypes despite lower GR. Morphotypes may have differing environmental niches that were not spanned by our experimental conditions. For instance, in a more oligotrophic and colder environment than ours, *S. natans* I dominated during 2014 and 2015 north of 24° N (Schell et al., 2015).

Future measurements of growth in contrasted conditions may help to explain field observations of morphotype composition and the dominance of *S. fluitans* III in the Caribbean.

3.3 *Significance of CNP and isotope composition*

Our results showed significant differences of %N, $\delta^{15}N$, $\delta^{13}C$ and C:N between morphotypes while no difference has been found between *S. natans* and *S. fluitans* in the large (n = 488) and long-term dataset of Lapointe et al. (2021). This discrepancy can be explained by the particular environmental history of our samples.

Overall, %N and %P% cannot explain the different GR among morphotypes. Both *S. fluitans* III and *S. natans* I have similar %N and %P values, but different GR. It may be related to nutrient uptake that occurred before the experiment.

The high N:P (30.33) and C:P value (827) of all morphotypes in our experiment suggests a limitation in P, as pointed out by Lapointe et al. (2021) for samples collected after 2010s. This P limitation may explain why %N differences do not result in growth rate variations.

The value of %C (23.5%) was low compared to the recent Mexican samples of Vázquez-Delfín et al. (2021). Conversely, %N values were high in agreement with the Lapointe et al. (2021) data for the 2010s, except for *S. natans* VIII which were lower in our study. The high C:N values (36) of *S. natans* VIII suggest that this morphotype was not in good growing conditions.

The isotopic composition showed high values in $\delta^{13}C$ which are footprints of the continental origin of C as a consequence of the coastal situation of our samples. The low values of $\delta^{15}N$ of *S. natans* I may be indicative of diazotrophic fixation, common in pelagic *Sargassum* (Carpenter, 1972; Phlips and Zeman, 1990) while higher values may indicate enrichment by NO_3^- present along the coast (Lapointe et al. 2021). It is interesting to note that $\delta^{15}N$ order among morphotypes follow the GR. This suggests that higher $\delta^{15}N$ indicate more recent growth fueled by coastal NO_3^-. That implies that the last growth of *S. natans* I was achieved at a greater distance in time and offshore.

Thus, the significant variations of the elemental composition point to a greater benefit for *S. fluitans* III from the coastal situation of our experiment than for the two *S. natans* morphotypes.

In conclusion, despite the non optimal conditions encountered in this experiment, it shows for the first time contrasting growth performances between morphotypes that are consistent with their abundance in the field. Current predictive models, which do not distinguish between morphotypes, can be improved by taking these growth differences into account. These differences in growth are probably linked to photosynthetic processes between morphotypes that will have to be specified with new experiments. *Sargassum fluitans* III appears here as the best candidate for cultivation, including indoors where access to light is more difficult.

4 Funding

This research has been supported by the French Agence Nationale de la Recherche Sargassum grants FORESEA (ANR-19-SARG-0007-01) and SAVE-C (ANR-19-SARG-0008) and by the French Institut de Recherche pour le Developpement Long-term Mission funding.

5 CRediT authorship contribution statement

Conceptualization, Data curation, Methodology, Software, Supervision, Validation, Visualization (TC, LB), Formal analysis (TC, LB, WP), Funding acquisition, Project administration, Resources (TC,LB, TT), Investigation (TC, TG), Writing (TC, LB, SC, VSP, TT).

6 Declaration of Competing Interest

None

7 Acknowledgements

We are grateful to Emmanuel Thouard, Ifremer Martinique, who gave access to Ifremer station facilities and meteorological data, Jean-Pierre Allenou, Ifremer Martinique, for the REPHY data and Samson Devillers, Ifremer Martinique, for his operational assistance. Tissue analysis was performed by PACEM Mediterranean Institute of Oceanography (MIO) intern platform. Patrick Raimbault, from the MIO, helped with interpretation. The map in Fig. S1 was partly produced by Felix Navarro MIO internship from AgroParisTech.

8 References

Aminot, A., Kérouel, R., 2007. Dosage automatique des nutriments dans les eaux marines: méthodes en flux continu. Ifremer, France.

Belin, C., Soudant, D., Amzil, Z., 2021. Three decades of data on phytoplankton and phycotoxins on the French coast: Lessons from REPHY and REPHYTOX. Harmful Algae 102, 101733. https://doi.org/10.1016/j.hal.2019.101733

Berline, L., Ody, A., Jouanno, J., Chevalier, C., André, J.-M., Thibaut, T., Ménard, F., 2020. Hindcasting the 2017 dispersal of Sargassum algae in the Tropical North Atlantic. Marine Pollution Bulletin 158, 111431. https://doi.org/10.1016/j.marpolbul.2020.111431

Brooks, M., Coles, V., Hood, R., Gower, J., 2018. Factors controlling the seasonal distribution of pelagic Sargassum. Mar. Ecol. Prog. Ser. 599, 1–18. https://doi.org/10.3354/meps12646

Carpenter, E.J., 1972. Nitrogen Fixation by a Blue-Green Epiphyte on Pelagic *Sargassum*. Science 178, 1207–1209. https://doi.org/10.1126/science.178.4066.1207

De Rock, P., Cimiterra, N., Allenou, J.-P., 2019. Réalisation d'un suivi du milieu marin en vue de la mise en oeuvre de la nouvelle station d'épuration (Pontaléry) au Robert - Caractérisation de l'état initial (Rapport Ifremer). Le Robert (Martinique).

García-Sánchez, M., Graham, C., Vera, E., Escalante-Mancera, E., Álvarez-Filip, L., van Tussenbroek, B.I., 2020. Temporal changes in the composition and biomass of beached pelagic Sargassum species in the Mexican Caribbean. Aquatic Botany 167, 103275. https://doi.org/10.1016/j.aquabot.2020.103275

Hanisak, M.D., Samuel, M.A., 1987. Growth rates in culture of several species of Sargassum from Florida, USA, in: Ragan, M.A., Bird, C.J. (Eds.), Twelfth International Seaweed Symposium. Springer Netherlands, Dordrecht, pp. 399–404. https://doi.org/10.1007/978-94-009-4057-4_59

Holmes, R.M., Aminot, A., Kérouel, R., Hooker, B.A., Peterson, B.J., 1999. A simple and precise method for measuring ammonium in marine and freshwater ecosystems. Can. J. Fish. Aquat. Sci. 56, 1801–1808. https://doi.org/10.1139/f99-128

Iporac, L.A.R., Hatt, D.C., Bally, N.K., Castro, A., Cardet, E., Mesidor, R., Olszak, S., Duran, A., Burkholder, D.A., Collado-Vides, L., 2022. Community-based monitoring reveals spatiotemporal variation of sargasso inundation levels and morphotype dominance across the Caribbean and South Florida. Aquatic Botany 182, 103546. https://doi.org/10.1016/j.aquabot.2022.103546

Johns, E.M., Lumpkin, R., Putman, N.F., Smith, R.H., Muller-Karger, F.E., T. Rueda-Roa, D., Hu, C., Wang, M., Brooks, M.T., Gramer, L.J., Werner, F.E., 2020. The establishment of a pelagic

241 Sargassum population in the tropical Atlantic: Biological consequences of a basin-scale long
242 distance dispersal event. Progress in Oceanography 182, 102269.
243 https://doi.org/10.1016/j.pocean.2020.102269
244 Jouanno, J., Benshila, R., Berline, L., Soulié, A., Radenac, M.-H., Morvan, G., Diaz, F., Sheinbaum, J.,
245 Chevalier, C., Thibaut, T., Changeux, T., Menard, F., Berthet, S., Aumont, O., Ethé, C., Nabat,
246 P., Mallet, M., 2021. A NEMO-based model of <i>Sargassum</i> distribution in the
247 tropical Atlantic: description of the model and sensitivity analysis (NEMO-Sarg1.0). Geosci.
248 Model Dev. 14, 4069–4086. https://doi.org/10.5194/gmd-14-4069-2021
249 Lapointe, B.E., 1995. A comparison of nutrient-limited productivity in Sargassum natans from neritic
250 vs. oceanic waters of the western North Atlantic Ocean. Limnol. Oceanogr. 40, 625–633.
251 https://doi.org/10.4319/lo.1995.40.3.0625
252 Lapointe, B.E., Brewton, R.A., Herren, L.W., Wang, M., Hu, C., McGillicuddy, D.J., Lindell, S.,
253 Hernandez, F.J., Morton, P.L., 2021. Nutrient content and stoichiometry of pelagic Sargassum
254 reflects increasing nitrogen availability in the Atlantic Basin. Nat Commun 12, 3060.
255 https://doi.org/10.1038/s41467-021-23135-7
256 Lapointe, B.E., West, L.E., Sutton, T.T., Hu, C., 2014. Ryther revisited: nutrient excretions by fishes
257 enhance productivity of pelagic Sargassum in the western North Atlantic Ocean. Journal of
258 Experimental Marine Biology and Ecology 458, 46–56.
259 https://doi.org/10.1016/j.jembe.2014.05.002
260 Machado, C.B., Maddix, G.-M., Francis, P., Thomas, S.-L., Burton, J.-A., Langer, S., Larson, T.R., Marsh,
261 R., Webber, M., Tonon, T., 2022. Pelagic Sargassum events in Jamaica: Provenance,
262 morphotype abundance, and influence of sample processing on biochemical composition of
263 the biomass. Science of The Total Environment 817, 152761.
264 https://doi.org/10.1016/j.scitotenv.2021.152761

Michotey, V., Blanfuné, A., Chevalier, C., Garel, M., Diaz, F., Berline, L., Le Grand, L., Armougom, F., Guasco, S., Ruitton, S., Changeux, T., Belloni, B., Blanchot, J., Ménard, F., Thibaut, T., 2020. In situ observations and modelling revealed environmental factors favouring occurrence of Vibrio in microbiome of the pelagic Sargassum responsible for strandings. Science of The Total Environment 748, 141216. https://doi.org/10.1016/j.scitotenv.2020.141216

Phlips, E., Zeman, C., 1990. Photosynthesis, growth and nitrogen-fixation by epiphytic forms of filamentous cyanobacteria from pelagic sargassum. Bulletin of Marine Science.

Powers, L.C., Hertkorn, N., McDonald, N., Schmitt-Kopplin, P., Del Vecchio, R., Blough, N.V., Gonsior, M., 2019. *Sargassum* sp. Act as a Large Regional Source of Marine Dissolved Organic Carbon and Polyphenols. Global Biogeochem. Cycles 33, 1423–1439. https://doi.org/10.1029/2019GB006225

Raimbault, P., Garcia, N., Cerutti, F., 2008. Distribution of inorganic and organic nutrients in the South Pacific Ocean – evidence for long-term accumulation of organic matter in nitrogen-depleted waters. Biogeosciences 5, 281–298. https://doi.org/10.5194/bg-5-281-2008

Schell, J., Goodwin, D., Siuda, A., 2015. Recent Sargassum Inundation Events in the Caribbean: Shipboard Observations Reveal Dominance of a Previously Rare Form. Oceanog 28, 8–10. https://doi.org/10.5670/oceanog.2015.70

Stoner, A., Greening, H., 1984. Geographic-variation in the macrofaunal associates of pelagic sargassum and some biogeographic implications. Mar. Ecol.-Prog. Ser. 20, 185–192. https://doi.org/10.3354/meps020185

Vázquez-Delfín, E., Freile-Pelegrín, Y., Salazar-Garibay, A., Serviere-Zaragoza, E., Méndez-Rodríguez, L.C., Robledo, D., 2021. Species composition and chemical characterization of Sargassum influx at six different locations along the Mexican Caribbean coast. Science of The Total Environment 795, 148852. https://doi.org/10.1016/j.scitotenv.2021.148852

289 Vranken, S., Robuchon, M., Dekeyzer, S., Bárbara, I., Bartsch, I., Blanfuné, A., Boudouresque, C.-F.,
290 Decock, W., Destombe, C., de Reviers, B., Díaz-Tapia, P., Herbst, A., Julliard, R., Karez, R.,
291 Kersen, P., Krueger-Hadfield, S.A., Kuhlenkamp, R., Peters, A.F., Peña, V., Piñeiro-Corbeira, C.,
292 Rindi, F., Rousseau, F., Rueness, J., Schubert, H., Sjøtun, K., Sansón, M., Smale, D., Thibaut, T.,
293 Valero, M., Vandepitte, L., Vanhoorne, B., Vergés, A., Verlaque, M., Vieira, C., Le Gall, L.,
294 Leliaert, F., De Clerck, O., 2022. AlgaeTraits: a trait database for (European) seaweeds
295 (preprint). ESSD – Ocean/Biological oceanography. https://doi.org/10.5194/essd-2022-329
296 Wang, M., Hu, C., Barnes, B.B., Mitchum, G., Lapointe, B., Montoya, J.P., 2019. The great Atlantic
297 *Sargassum* belt. Science 365, 83–87. https://doi.org/10.1126/science.aaw7912
298

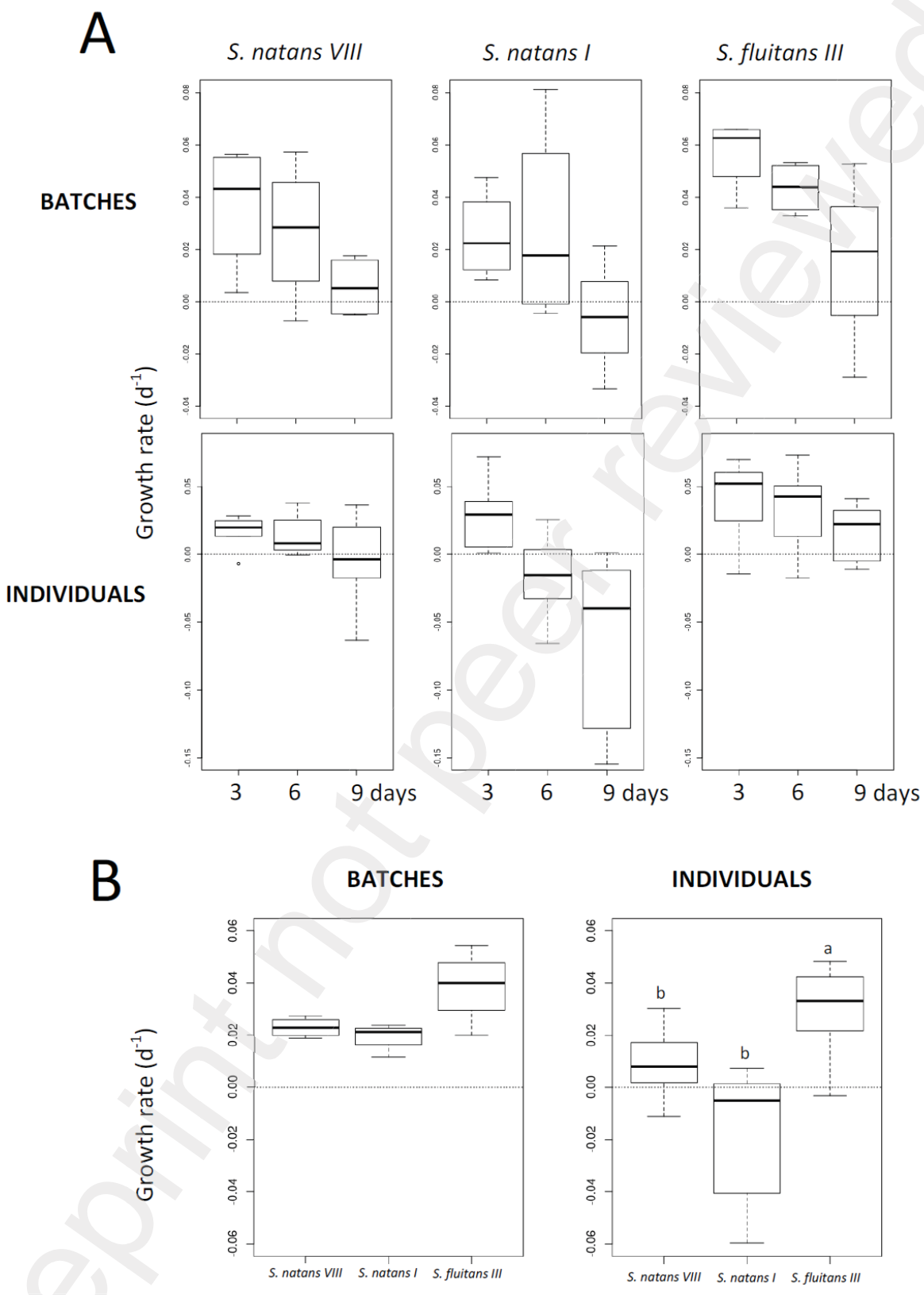

299

300 Fig. 1: Holopelagic *Sargassum* growth rate (d^{-1}) for each morphotype measured on batches (n=4) and

301 individuals (n=12 per morphotype) every 3 days (A.) and over the 9 days of the experiment (B.). Box

302 shows the sample median and the first and third quartiles. Whiskers extend to the last data point

which is no more than 1.5 times the interquartile range. Outliers are shown as dots. The letter identifies the significant differences (p-value<0.05).

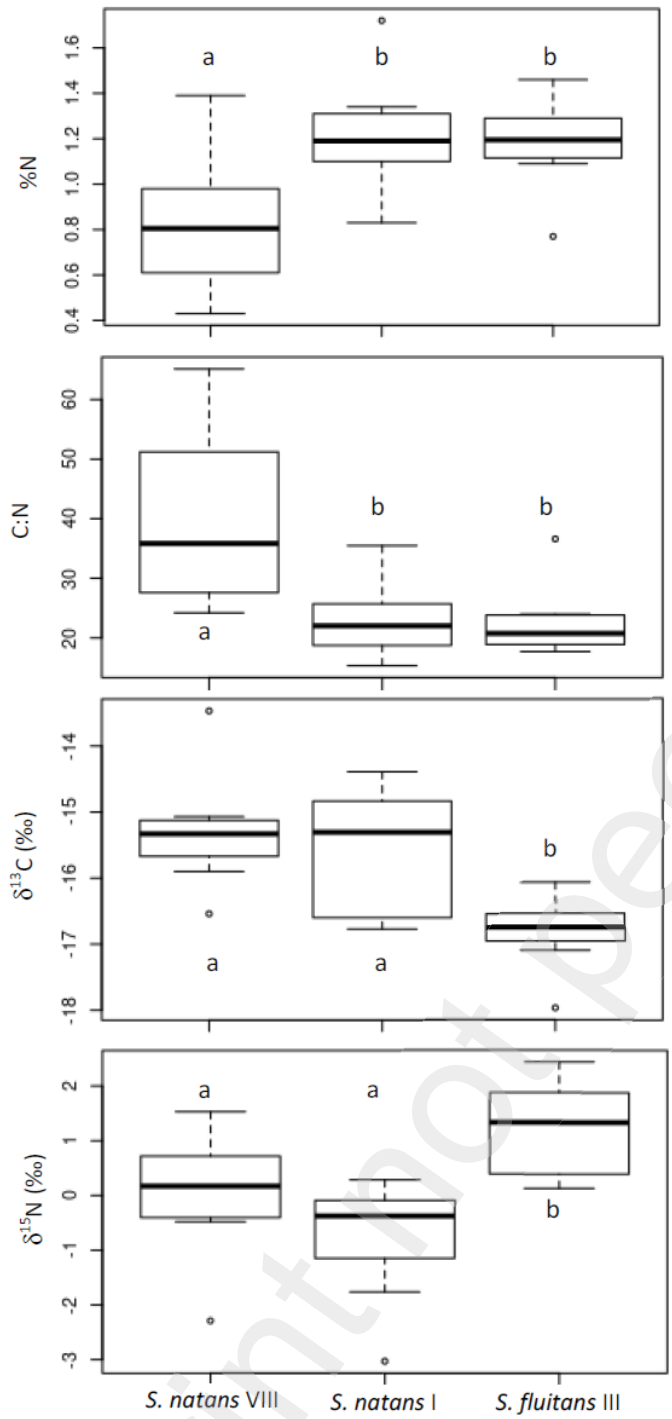

306

307 Fig. 2: Tissue composition (%N, C:N, $\delta^{15}N$, $\delta^{13}C$) between *Sargassum* morphotypes. Box, whiskers and

308 letters are shown as in Fig. 1.

Supplementary material of Growth and tissue composition (CNP, isotopes) of the three morphotypes of pelagic sargassum

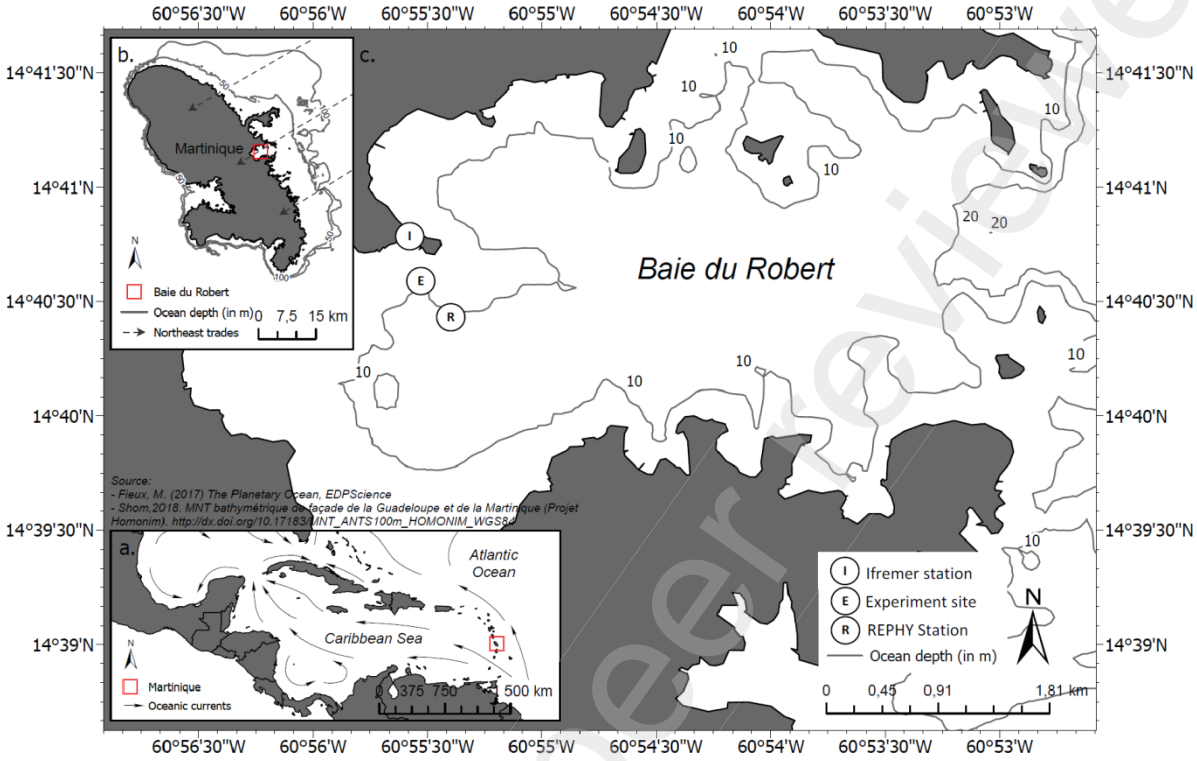

Fig. S1: Location of Ifremer station (I), experimental site (E) and REPHY monitoring station (R) with bathymetry. (a.) Regional position of Martinique Island, framed in red, with the main oceanic currents. (b.) Martinique Island with the orientation of the trade winds and location of Baie du Robert framed in red.

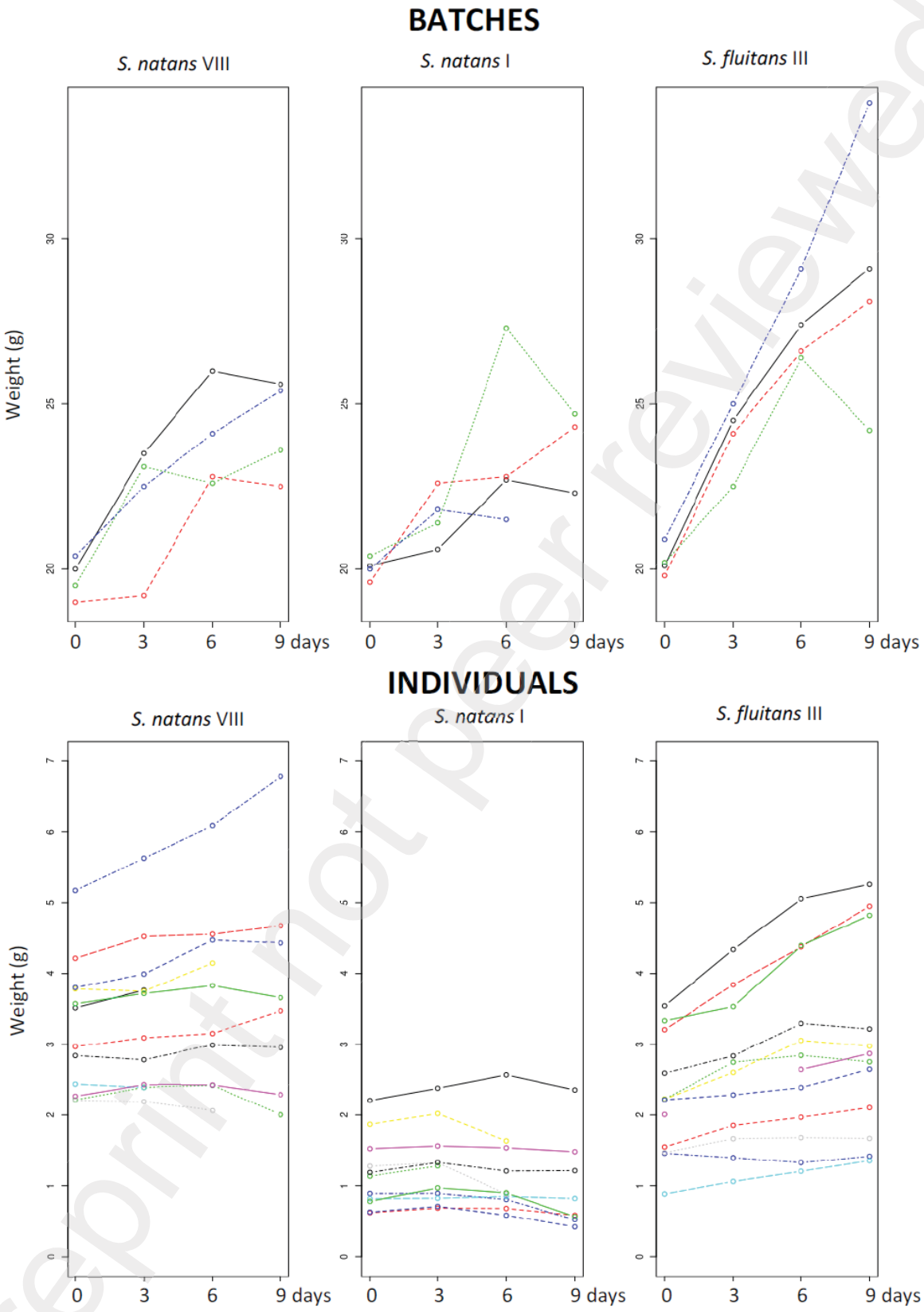

Fig. S2: *Sargassum* wet weight patterns of change over time for measurements of batches (n = 4) and individuals considering the different morphotypes (*S. natans* VII (n = 12), *S. natans* I (n = 12), and *S. fluitans* III (n = 12). Each line is a batch or an individual. It can be interrupted when a mark was lost or an apex dead or an individual broken in two parts.

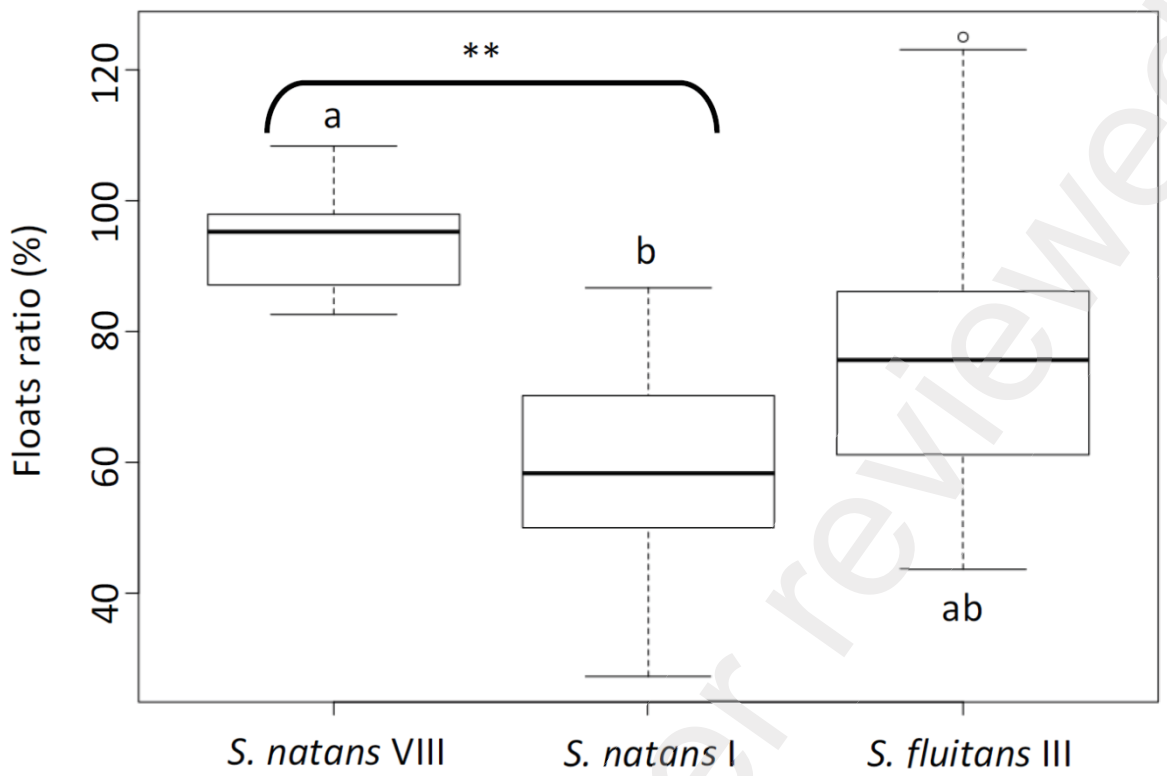

Fig. S3: Floats ratio after 9 days for the 3 morphotypes. Box shows the sample median and the first and third quartiles. Whiskers extend to the last data point which is no more than 1.5 times the interquartile range. Outliers are shown as dots. The KW test χ^2= 10.76, df = 2, p-value = 0.004608. The only significant Dunns post hoc test is between *S. natans* VIII vs *S. natans* I (p=0.00104**). Note that some individuals *S. fluitans* III and *S. natans* VII show values over 100% since they have more floats at the end of the experiment than at the beginning.

Table S1: Synthesis of Kruskal-Wallis and Dunns post hoc test results for the morphotype effect on *Sargassum* composition in %C, %N, %P, C:N, N:P, C:P, δ^{15}N, δ^{13}C.

	%C	%N	%P	C:N	N:P	C:P	δ13C	δ15N
Kruskal Wallis Chi2	3,62	6,635	5,235	10,955	1,28	0,335	11,115	11,185
df	2	2	2	2	2	2	2	2
p-value	0,164	0,036	0,073	0,004	0,527	0,846	0,004	0,004
Dunns p-value *S. natans* VIII *vs S. natans* I		0,022		0,005			0,671	0,179
Dunns p-value *S. natans* VIII *vs S. fluitans* III		0,031		0,003			0,002	0,048
Dunns p-value *S. natans* I *vs S. fluitans* III		0,888		0,888			0,008	0,001
Median	23,52%	1,14%	0,07%	23,85	30,33	827,43	-15,99	0,16
Median *S. natans* VIII		0,80%		35,86			-15,33	0,17
Median *S. natans* I		1,19%		22,03			-15,31	-0,38
Median *S. fluitans* III		1,20%		20,76			-16,75	1,33